Transcriptome analysis reveals rice OsMADS13 as an important repressor of the carpel development pathway in ovules

Highlight: Transcriptome analysis of the rice *osmads13* mutant

author for contact: Martin M. Kater

Michela Osnato[1,2], Elia Lacchini[1,3], Alessandro Pilatone, Ludovico Dreni[1,4], Andrea Grioni, Matteo Chiara[1], David Horner[1], Soraya Pelaz[2] and Martin M. Kater[1].

[1]Department of Biosciences, University of Milan, Via Celoria 26, 20133 Milano (ITALY). [2]Centre for Research in Agricultural Genomics (CRAG), CSIC-IRTA-UAB-UB, Campus UAB, Barcelona (SPAIN). [3]VIB Center for Plant System Biology, Ghent (BELGIUM). [4]Instituto de Biología Molecular y Celular de Plantas, Consejo Superior de Investigaciones Científicas-Universidad Politécnica de Valencia, Valencia (SPAIN)

Corresponding author: Martin M. Kater, martin.kater@unimi.it

Abbreviations: SAM, FM, OP, TF, DEG, TE, LMD

ABSTRACT

In angiosperms, floral homeotic genes encoding MADS-domain transcription factors regulate the development of floral organs. Specifically, members of the SEPALLATA (SEP) and AGAMOUS (AG) subfamilies form higher order protein complexes to control Floral Meristem determinacy and to specify the identity of female reproductive organs. In rice, the *AG* subfamily gene *OsMADS13* is intimately involved in the determination of ovule identity, since knock-out mutant plants develop carpel-like structures in place of ovules resulting in female sterility. Little is known about the regulatory pathways at the base of rice gynoecium development. To further investigate molecular mechanisms acting downstream of OsMADS13, we obtained transcriptomes of immature inflorescences from wild type and the *osmads13* mutant. Among a total of 476 Differentially Expressed Genes (DEGs), a substantial overlap with DEGs from the *SEP*-family *osmads1* mutant was found, suggesting that OsMADS1 and OsMADS13 may act on a common set of target genes. Expression studies and preliminary analyses of two upregulated Zinc-finger transcription factor encoding genes indicate that our dataset represents a valuable resource for the identification of both OsMADS13 target genes and novel players in rice ovule development. Taken together, our study suggests that OsMADS13 is an important repressor of the carpel pathway during ovule development.

Keywords: gynoecium, floral meristem determinacy, ovule, transcription, rice

INTRODUCTION

In the majority of angiosperms studied so far, the formation of different floral organs in four concentric whorls is genetically controlled by five classes of transcription regulators (reviewed by Bowman et al., 2012). The ABCDE model suggests that A- and B-class transcription factors (TFs) determine the development of sepals and petals in the outermost whorls, whereas B- and C- class TFs control the formation of stamens and carpels in the innermost whorls (Causier et al., 2010). Additional D-class factors exert their function in the formation of the ovule, the specialized sporophytic structure enclosing the female gametophyte which, upon fertilization, gives origin to the seed (Pinyopich et al., 2003; Dreni et al., 2007). Finally, E-class factors are required for the development of all floral structures and represent a molecular hub, as they mediate the formation of homo/heteromeric regulatory complexes composed of different combination of A-, B-, C-, or D-class factors specific to each of the four whorls (Malcomber and Kellogg, 2005). The majority of these floral homeotic proteins belong to the MADS-domain family and have been proposed to operate as quartets (two interacting dimers; reviewed by Theißen and Saedler, 2001) that bind two cis-regulatory elements, known as CArG-boxes, in the promoters of the genes that they regulate (Egea-Cortines et al., 1999; Mendes et al., 2013). This genetic model is broadly conserved across flowering plants, although variations are associated with a range of flower morphologies (Theissen and Melzer, 2007).

In the model species *Arabidopsis thaliana*, the floral meristem (FM) gives rise to four sepals, four petals, six stamens and two fused carpels. Four E-class factors SEPALLATA (SEP) 1, SEP2, SEP3 and SEP4 act redundantly to determine the identity of all floral organs (Pelaz et al., 2000; Ditta et al., 2004), and a complex composed of E-class and the C-class factor AGAMOUS (AG) specifies the identity of stamens and carpels, and controls FM determinacy (Bowman et al., 1989). The FM is consumed during flower development as AG regulates the shift towards organogenesis by mediating direct and indirect repression of the stem cell identity gene *WUSCHEL* (*WUS)* in the FM (Laux et al., 1996; Brand et al., 2000; Schoof et al., 2000; Sun et al., 2009; Liu et al., 2011).

In the Arabidopsis genome, three additional *AG-like* genes - *SHATTERPROOF1* (*SHP1*), *SHP2* and *SEEDSTICK* (*STK*) - are named after their function in seed dispersal (Liljegren et al., 2000; Pinyopich et al., 2003; Balanzà et al., 2016). Although *STK* is specifically expressed in the pistil and ovules, the loss of its function only affects the formation of funiculi (Pinyopich et al., 2003; Mizzotti et al., 2014). However, integuments are converted into carpelloid structures in the *shp1 shp2 stk* triple mutant, indicating that the three genes act redundantly in the determination of ovule identity (Pinyopich et al., 2003; Brambilla et al., 2007). Interestingly, the formation of carpel-like organs in the place of

ovules was also observed in the *sep1 sep2 sep3/+* triple mutant (Favaro et al., 2003), demonstrating that these factors are crucial for a correct reproductive development. At the molecular level, STK, SHP1, and SHP2 redundantly control the expression of *VERDANDI* (*VDD*), a gene encoding a B3-domain transcription factor involved in the development of antipodal cells and synergids (Matias-Hernandez et al., 2010). Specifically, the STK-SEP3 dimers bind two nearby CArG boxes in the promoter of *VDD,* inducing the formation of a loop which results in the activation of *VDD* in the female gametophyte (Mendes et al., 2013). In the pistil STK interacts with NO TRANSMITTING TRACT (NTT) to control early events of gynoecium development and septum function which is important for fertilization (Herrera-Ubaldo et al., 2019). Moreover, STK also plays a role in fruit development by regulating the cytokinin hormonal pathway, thus controlling fruit size (Di Marzo et al., 2020).

In grasses, the duplication and diversification of *MADS-box* genes is likely associated with the origin and diversification of flower morphology (the spikelet; Malcomber and Kellogg, 2004). In rice (*Oryza sativa*), the floret meristem differentiates the palea and lemma, two lodicules (equivalent to petals), six stamens and a central carpel containing a single ovule (Itoh et al., 2005). Among the five *SEP-like* genes in the rice genome, the *OsMADS1* loss of function mutant, originally described as *leafy hull sterile 1* (*lhs1*), displays defects in both flower development and FM determinacy, resembling E-class function mutants (Jeon et al., 2000). Indeed, in *osmads1* mutants, floral organs are converted into glume-like structures, and a spikelet-within-a-spikelet develops in the centre of the flower (Jeon et al., 2000; Prasad et al., 2001; Agrawal et al., 2005; Prasad et al., 2005; Hu et al., 2015a). Similar to Arabidopsis, the rice AG homologs OsMADS3 and OsMADS58 redundantly control the identity of reproductive organs (stamens and carpels) and meristem determinacy (Yamaguchi et al., 2006; Dreni et al., 2011). Also the AG-like factor OsMADS13 controls the determinacy of the floral meristem and the identity of the ovule within the carpel thus showing a class D function, since *osmads13* mutants display homeotic transformations of ovules into carpels (Dreni et al., 2007; Dreni et al., 2011).

In the last decade, large scale omics approaches have facilitated a deeper understanding of Gene Regulatory Networks (GRNs) underlying flower development, particularly in Arabidopsis. ChIP-sequencing and transcriptomics analyses have helped in deciphering the transcriptional cascades downstream of the C-class factor AG (Ó'Maoiléidigh et al., 2013) and the E- class factor SEPALLATA 3 (Kaufmann et al., 2009). These studies suggest a function of AG in the promotion of gynoecium development via the activation of auxin biosynthesis (Ó'Maoiléidigh et al., 2013; Yamaguchi et al., 2017), and of SEP3 in the regulation of floral organ morphogenesis via auxin signalling pathways (Kaufmann et al., 2009).

The combination of genome-wide DNA binding assays and expression data also indicate that the rice E-class factor OsMADS1 activates genes in the auxin pathway involved in the differentiation of female reproductive tissues (Khanday et al., 2013; Khanday et al., 2016). Nevertheless, genetic and molecular studies suggest a complex interplay between rice floral homeotic factors (Li et al., 2011; Hu et al., 2015a). Transcriptomic analyses also provided valuable information regarding different steps of male and female gamete development in rice (Tang et al., 2010; Kubo et al., 2013). However, little is known about the molecular mechanisms underlying the gene regulatory networks controlling ovule development in rice.

Here we investigated changes in the modulation of gene expression between wild-type and the *osmads13* mutant, identifying genes that were deregulated in developing *osmads13* inflorescences. By comparing our datasets with those published for *OsMADS1* knock-down and knock-out mutants (Khanday et al., 2013; Hu et al., 2015), we identified interesting regulatory genes and performed detailed expression analyses in specific cell types and functional characterization during reproductive growth. Taken together, our findings provide new insights into the early processes regulating the formation of female reproductive organs. Based on these findings, we propose a genetic framework downstream of the D-class factor OsMADS13.

MATERIALS AND METHODS

PLANT MATERIAL and GROWTH CONDITIONS

Rice (*Oryza sativa L. ssp. Japonica*) plants were grown under controlled conditions in a LD chamber (16 h light at 28°C, 8 h dark at 22°C). After 8-10 weeks, plants were transferred to a SD chamber (10 h light at 28°C, 14 h dark at 22°C) to induce flowering. Developing inflorescences (0.5-0.7 cm length) were harvested 3 weeks after the LD-SD shift for expression analysis. As previously described (Itoh et al. 2005), these stages correspond to In6 and In7 of inflorescence development, Sp7 and Sp8 of spikelet development (carpel primordium the former, ovule and pollen the latter), and Ov1 of ovule development. After heading, mature flowers at anthesis were collected for phenotypic analysis.

In this study, we used *osmads13* Tos17 insertion mutant (cv Dongjin) in a heterozygous state since homozygous mutants are female-sterile (Dreni et al., 2007). Segregating progenies of *osmads13* heterozygous plants were genotyped by duplex PCR, and only wild-type and homozygous mutants were analysed. The Rice Functional Genomic Express Database (http://signal.salk.edu/cgi-

bin/RiceGE) was searched for mutations in candidate genes, and T-DNA insertion lines were obtained from Postech. Primers used for genotyping are reported in **Supplementary Table S1.**

Total RNA Extraction and RNA-sequencing

Total RNA was extracted from pools of developing inflorescences (In6 and In7 stages) using the Pure Link RNA MiniKit (AMBION). Three biological replicates were collected for the two genotypes. RNA quality and quantity were assessed by gel electrophoresis, BioAnalyzer and Nanodrop. Upon treatment with TURBO DNAse I (AMBION), 4 µg of RNA were used to produce sequencing libraries with the TruSeq mRNA sample preparation kit. Sequencing of poly(A) RNA samples was carried out in multiplex (6 samples per lane, single 50 bp reads for 20 M each sample) with Illumina Hi-seq 2000 platform at IGA Technology Services (Udine, Italy).

RNA-sequencing analysis

Gene expression levels were estimated by using the standard Bowtie-Tophat-Cufflinks pipeline (Trapnell et al., 2013) on the established gene model of the Rice Genome Annotation (MSU 7.0 non TE release) (Kawahara et al., 2013), without performing a de novo assembly of the transcriptome. Differential expression analyses were performed by DESeq (Bioconductor version, Release 2.12), and only genes with a false discovery rate (FDR) lower than 0.05 were considered. Following GO-slim annotation, enrichment tests were performed using the AgriGO analysis toolkit (Du et al., 2010), with a custom background formed only by expressed genes (FRPKM>=1).

Raw sequencing data produced in this study have been deposited at the NCBI short read archive (SRA) under the PRJNA638800 accession. Gene expression patterns of wild-type and *OsMADS1* loss of function mutant inflorescences were retrieved from GSE62078, GSE62078, GSE62078, GSE62078, GSE62078, GSE62078, GSE62078. Venn diagrams of overlapping gene lists were generated with tools available at http://bioinformatics.psb.ugent.be/cgi-bin/liste/Venn/calculate_venn.htpl. For selected candidate genes, information on paralogous and orthologous genes were retrieved using http://gramene.org/, whereas transcription domains were inferred exploring http://ricexpro.dna.affrc.go.jp.

Sample collection and preparation for Laser-assisted Micro-Dissection (LMD)

Developing inflorescences were collected and fixed under vacuum with Acetone for 15 minutes. The fixative was replaced, and the samples left at 4°C overnight. For infiltration, acetone was replaced first with acetone/xylene series and then by molten Paraplast Xtra (Sigma-Aldrich) with 2 hours changes for 24 hours at 54°C. Embedded samples were stored at 4°C. Frame slides (PET Membrane) and stands for LMD were sterilised by irradiation with UV light for 30 minutes using a UV cross-linker (Stratalinker 1800, Stratagene).

Embedded samples were cut in 10 µm sections on a rotary microtome, and ribbons were stretched on treated Frame Slides with methanol for a maximum of 30 minutes at 37°C (under chemical hood). Prior LMD, slides were immersed twice in xylene (5 minutes each) to dissolve paraffin, and then air-dried for 5 minutes at room temperature. For each sample, 80-100 cuts were obtained using the LMD 6000 system equipped with Axiovert 200. All the materials used were provided by Leica Microsystems. Membrane-bound cells were collected into 0.5 ml tube caps (low-bind Eppendorf) and resuspended in Extraction Buffer (see below). After 30 minutes incubation at 42°C, samples were stored at -80°C.

RNA extraction from specific cell types and cDNA amplification

Total RNA was extracted from pools of specific cell types using the PicoPure RNA isolation kit according to the manufacturer's instructions (Arcturus). Genomic DNA was removed using DNAse I (QIAGEN) on column during RNA extraction procedure. The integrity of extracted RNA samples was assessed by using the RNA 6000 Pico assay kit on 2100 BioAnalyzer (Agilent Technologies). The RNA Integrity Number (RIN) of our samples ranged from 7.10 to 7.40, of acceptable quality for down-stream application (Takahashi et al., 2010). Due to the low quantity of starting material, 50 ng of total RNA extracted from microdissected materials were used to produce up to 5 µg of amplified cDNA using the Ovation Pico SL WTA System V2 following the manufacturer's instructions (NuGEN).

Expression analysis

For standard RT-qPCR, RNA samples were treated with DNaseI RNase free (Ambion) and retro-transcribed with ImProm system (Promega). cDNA samples were used in qPCR reactions using iQ SYBR Green SuperMix on CFX96 Real Time System (BIORAD).

High-throughput qPCR was carried out using the Microfluidic Dynamic Array developed by Fluidigm Corporation (Spungeon et al., 2008). A fast cycling protocol was used on BioMark machine by using EvaGreen (BIO-RAD) as dye. The experiment was performed at the Genomics Platform of CRAG (Barcelona, SPAIN), following the workflow provided by the manufacturer. For each sample, 3 Technical Replicates were performed and data were normalized using *OsEF1* or *OsUBQ*.

Relative expression levels are reported as mean values of three biological replicates, with error bar representing the standard deviation (SD). For each experiment, statistical significance was determined comparing two columns (wild-type versus mutant) by using unpaired Student's two-tailed t test, with confidence interval at 95%. Primers used for standard and large-scale qPCR are reported in **Supplementary Table S2**.

In situ hybridization was performed as previously described (Dreni et al., 2007).

Phenotypic analyses of transgenic lines

Morphological analyses of reproductive organs - dissected from mature flowers at anthesis of different transgenic lines and wild-type control - were carried out by using a Zeiss Axiophot D1 microscope outfitted with a Zeiss AxioCam MR camera. Samples for histological analysis and whole-mount tissue clearing were prepared as previously described (Dreni et al., 2007; Dreni et al., 2011).

Longitudinal thin sections (5-µm-thick) of wild-type and *dst* mutant mature pistils, previously embedded in Technovit resin, were stained with 0.1% Toluidin blue and mounted with a coverslip.

Images of developing ovaries (dissected from wild-type plants and transgenic lines carrying OsMADS13-GFP fusion) were taken in bright field and under UV light to observe alteration in stigma formation and detect the GFP signal in transgenic lines.

Analysis of putative regulatory sequences of DEGs

AGAMOUS-like binding sites (**CC** $(A/T)_{5-7}$ **GG)** were searched in the loci of interest (3 kb upstream of the Transcription Start Site, exons, introns, 5' and 3' UTRs) by using TRANSFAC website (http://gene-regulation.com/pub/databases.html). Based on previous findings, two criteria were followed: regulatory sequences must contain maximum one mismatch in the CG clamp or in the A/T core, and at least two CArG-boxes within 600 bp.

Direct binding of OsMADS13 to downstream genes.

To generate the set of reporter vectors, different promoter regions of *DL, ZOS3-19/DST* and *OsZHD8* were cloned as SalI-PstI fragments in a modified pGreenII 0800-LUC carrying *Pro35S:LUC* and *Pro35S:REN* (as internal control to estimate the proportion of transformed protoplasts). Protoplasts were isolated from rice calli by digesting the cell-wall with Macerozyme R-10 and Cellulase (Yakult Pharmaceuticals). Different combinations of effector (*Pro35S:OsMADS13)* and reporter vectors were co-transfected using PEG. After 18 hours incubation in darkness at 24°C, transformed protoplasts were pelleted and resuspended in homogenization buffer for RNA extraction. Transactivation activity of OsMADS13 was assessed by RT-qPCR by calculating the relative ratio of mRNA abundance of *Luciferase* and *Renilla* reporter genes. Data are reported as mean values of three biological replicates, with error bar representing the standard error of the mean (SEM). Statistical significance was determined comparing two columns (with and without the OsMADS13 effector) by using unpaired Student's two-tailed t test, with confidence interval at 95%. Primers used for transient assays are reported in **Supplementary Table S3**.

RESULTS

Transcriptome analysis of *osmads13* mutant vs wild type during flower development

We grew wild-type and *osmads13* mutant rice plants for eight weeks under Long Days (LD) and then transferred them to Short Days (SD) to induce flowering. In these conditions, floral transition took place within one week from the LD to SD shift, whereas the formation and differentiation of floral organs began two weeks after induction in a basipetal fashion (Itoh et al., 2005). Under these experimental conditions, developing inflorescences are characterized by a gradient of floral organ formation: early stages being at the bottom whereas late stages are at the top. Macroscopic differences between wild type and *osmads13* mutant became visible only once floral organs were fully formed. While ovules developed in wild-type florets, ectopic carpels developed in place of ovules in *osmads13* florets (Dreni et al., 2007). RNA-sequencing analysis using whole immature inflorescences was performed to identify genes that are deregulated in the *osmads13* mutant.

Developing inflorescences (5-8 mm long) were harvested from wild-type and mutant plants three weeks after the LD to SD shift, total RNA was extracted and poly(A)-selected libraries were sequenced. Reads were mapped to the reference genome of *Oryza sativa subspecies japonica* cv

Nipponbare (details in Materials and Methods) and the transcriptional profiles of wild-type and *osmads13* were compared. We identified a total of 811 differentially expressed genes (DEGs) (p-value <=0.05) in *osmads13*. This number was further reduced to 476 genes when the Benjamini-Hochberg technique for the control of the False Discovery Rate (FDR) was applied (cut-off of 0.05; **Data Set I**). Annotation of the 476 DEGs based on the GO-slim ontology suggested that 11 DEGs were related to Transposable Elements (TE), 80 encoded proteins with unknown function leaving 376 DEGs with assigned functions (**Fig. 1A)**. Subsequently, we divided the latter group into the following functional categories (**Fig. 1B)**: metabolism (31%), Nucleic Acid Binding (26%), Protein binding (17%), structural components (16%), and response to endogenous and exogenous stimuli (10%)**.**

Gene Ontology (GO) enrichment analyses, which were executed using the whole set of expressed genes as the background, identified "DNA binding" and "transcription regulator activity" as the most over-represented ontologies in the molecular function class; conversely, the term "catalytic activity" was under-represented (**Fig. 1C).** Interestingly, we observed a high enrichment of the GO-term "Transcription Factor activity" (**Supplementary Fig. S1A)**, especially when only DEGS upregulated in *osmads13* (**Supplementary Fig. S1B)** were considered. In contrast, categories related to "protein binding" were over-represented in the group of genes downregulated in *osmads13* (**Supplementary Fig. S1C)**.

Regarding genes related to transcription regulation, the most represented TF families were APETALA2 and Zinc-Finger (22%), followed by MYB (11%), Homeo-Domain (9%), basic Helix-Loop-Helix and basic Leucine Zipper (7%), Heat Shock Factors and No Apical Meristem (4%), as reported in **Fig. 1D.** Surprisingly, 83% of the DEGs encoding DNA binding proteins (67/81 genes) were upregulated in *osmads13* compared to the 53% of the DEGs with an annotated function (199/375 genes), suggesting a de-repression of regulatory genes in *osmads13* inflorescences.

Known regulators of reproductive development are deregulated in *osmads13*

OsMADS13 is activated slightly before ovule primordia (OP) arise in the centre of the carpel and remains expressed throughout all stages of ovule development (Lopez-Dee et al., 1999; Dreni et al., 2007). We used Laser assisted Micro-Dissection (LMD) followed by RT-qPCR to monitor changes in the expression of selected genes in specific cell types such as FM and OP isolated from wild-type and *osmads13* mutant flowers (**Supplementary Fig. S2)**.

The stages and quality of the LMD tissues were assessed by monitoring the relative expression levels of the ovule identity gene *OsMADS13*, together with known genes involved in carpel development. As expected, *OsMADS13* transcripts were almost undetectable in mutant plants (**Fig. 2A**). In contrast, *DROOPING LEAF* (*DL*), a gene normally expressed in carpel tissue (Yamaguchi et al., 2004), was upregulated in the *osmads13* mutant (**Fig. 2B**). This observation is consistent with previous analyses based on *in situ* hybridization, showing ectopic transcription of *DL* in carpel-like organs of homeotic mutants (Dreni et al., 2007; Li et al., 2011). Here, a 10-fold increase of *DL* expression is detected in *osmads13* at early stages of flower formation, specifically in the cell types that are committed to differentiate into the ectopic carpels that replace the ovule in the mutant (**Fig. 2B**). We also observed increased levels of the *AG* subfamily genes *OsMADS3* (**Fig. 2C)** and *OsMADS58* (**Fig. 2D),** which are involved in carpel development. Conversely (**Fig. 2E)**, we found decreased mRNA levels for the *LEAFY-like* gene *ABERRANT PANICLE ORGANIZATION* 2 (*APO2*) and the *ARGONAUTE-like* (*AGO*) gene *MEIOSIS ARRESTED AT LEPTOTENE1 (OsMEL1),* which both encode factors involved in ovule and germ cell development (Nonomura et al., 2007; Ikeda-Kawakatsu et al., 2012). Taken together, these results support the hypothesis that in ovule primordia OsMADS13 might directly or indirectly repress carpel identity genes (*DL*, *OsMADS3*, and *OsMADS58)* and activate genes involved in ovule development (*APO2* and *OsMEL1).* This observation is coherent with the observed *osmads13* mutant phenotype.

Notably, we observed that *OsFD1/OsbZIP77* and *OsSPL14*, two regulatory genes with known roles in the control of meristematic activity during inflorescence development, remained expressed during flower development and were upregulated in *osmads13* primordia as compared to wild-type (**Supplementary Fig. S3**). *OsFD1/OsbZIP77* is involved in the transition from vegetative to reproductive meristem (Taoka et al., 2011), while *OsSPL14* determines the formation of primary and secondary branches of the inflorescence meristems (Jiao et al., 2010; Miura et al., 2010). Therefore, the regulatory activity of *OsMADS13* seems to extend to the repression of genes that are otherwise expressed throughout the reproductive phase.

Candidate genes expressed in reproductive tissues are deregulated in *osmads13*

We used RT-qPCR to perform an additional validation of the RNA-seq results on a selection of DEGs without previously known function in gynoecium development. Among the genes downregulated in the mutant, we chose *OsbZIP52* (also known as *Rice Seed bZIP5*, *RBZ5*) due to its high expression after fertilization according to RiceXPro database (**Supplementary Fig S4**). We also analysed the expression of two loci (LOC_Os02g13800 and LOC_Os09g35790) encoding Heat Stress Transcription Factors (HSFs), and one locus (LOC_Os01g08860) encoding a Heat Shock Protein (HSP-like20). This

choice was based on the evidence that chaperone activity was overrepresented in the group of downregulated genes in the *osmads13* mutant (**Supplementary Fig S1C**). For these four genes, we confirmed decreased transcript levels in *osmads13* inflorescences **(Fig. 3A)**; however, only *HSP-like20* was also downregulated in *osmads13* ovule primordia **(Fig. 3B).**

Among the genes upregulated in the mutant, we focused our analysis on interesting candidates belonging to the basic Helix-Loop-Helix (bHLH) superfamily. This broad group of transcription regulators are involved in different developmental processes in numerous eukaryotic organisms (Massari and Murre, 2000). The first candidate gene, LOC_Os04g23550 *(OsbHLH6*), belongs to a cluster of *bHLH* genes which includes *UNDEVELOPED TAPETUM* (*UDT1*, Jung et al., 2005) and *TAPETUM DEGENERATION RETARDATION* (*TDR*, Li et al., 2006), two important regulators of pollen development (**Supplementary Fig. S5A**). Besides in anthers, *OsbHLH6* also seems to be expressed in reproductive meristems (**Supplementary Fig. S5B**), developing carpels and ovaries after pollination (**Supplementary Fig. S5C**). This gene has 2 putative splicing isoforms differing in length, with the shorter lacking the basic domain necessary for DNA binding (i.e., the first two exons and the second intron of the longer variant are included in the 5' UTR of the shorter variant). Specific primers were designed to discriminate between the two alternatively spliced transcripts (**Fig. 3C**). Expression analysis using primers amplifying the 3' end of *OsBHLH6* (common for both variants) revealed strong upregulation of this gene in inflorescence and ovule primordia in the *osmads13* mutant (**Fig. 3D**). Conversely, the use of primers specific to *OsbHLH6.2* revealed almost complete absence of the shorter transcript in all tissues tested (**Fig. 3E**), indicating little or no contribution to the mRNA abundance for this locus by the short splicing variant.

A second candidate gene, *LOC_Os01g50940* (*OsbHLH10*) was found to cluster together with *MYC2-like* genes (Fernández-Calvo et al., 2011; **Supplementary Fig. S6**), and specifically with *JASMONATE ASSOCIATED MYC2-like* loci (JAMs), encoding transcriptional repressors involved in JA response (Sasaki-Sekimoto et al., 2013) and male fertility (Nakata and Ohme-Takagi, 2013). The expression of this gene was almost undetectable in FM of wild-type and mutant but was strongly up-regulated in inflorescences and ovule primordia of the *osmads13* mutant (**Fig. 3F**).

The final candidate, LOC_Os09g24490 (*OsbHLH39*), was selected as it shares common features with the *TARGET of MONOPTEROS 5* (*TMO5)* and *TMO5-like*, described as important regulators of lateral organ formation such as roots and ovules in Arabidopsis (Moreno-Risueño et al., 2010; Galbiati et al., 2013); **Supplementary Fig. S7**). *OsbHLH39* was highly expressed during reproductive development and was upregulated in all mutant tissues tested (**Fig. 3G**).

Overlapping transcriptomes of D- and E- class loss of function mutants

In Arabidopsis, SEP and AG proteins form dimers to control the identity of carpels and ovules in the innermost whorl of developing flowers (Honma and Goto, 2001; Favaro et al., 2003). Recent analyses also showed that SEP3 and AG can form tetramers to control a subset of target genes involved in FM determinacy (Hugouvieux et al., 2018).

Moreover, previous molecular and genetic studies of floral homeotic factors in rice indicated a network of complex molecular interactions between members of these two subfamilies (Cui et al., 2010; Hu et al., 2015). To gain deeper insights into the possible interplay between D- and E-class factors during gynoecium development, we compared the list of DEGs in the immature inflorescences of *osmads13* with the collection of genes deregulated in a *OsMADS1* knock-down (*OsMADS1* RNAi) and knock-out (*osmads1-z*) plants (Khanday et al., 2013; Hu et al., 2015). Interestingly, half of the DEGs in *osmads13* were also deregulated in *OsMADS1-i* and/or in *osmads1-z* inflorescences (**Dataset II).** Precisely, 67% of genes up-regulated in *osmads13* (131/197, group I) were down-regulated in *osmads1* loss of function mutants (**Fig. 4A)**, and 33% of genes down-regulated in *osmads13* (59/177, group II) were up-regulated in *osmads1* loss of function mutants (**Fig. 4B).** GO test for biological processes of group I revealed significant enrichment for the term "response to endogenous stimulus" and "signal transduction" (**Fig. 4C),** consistent with the function of OsMADS1 and OsMADS13 in regulating flower development. The same analysis for group II revealed enrichment of the "photosynthesis and generation of precursors and metabolite" terms (**Fig. 4D**). This last observation is likely due to the conversion of all floral organs into green photosynthetic tissues (glume-like organs) in *osmads1* loss of function mutants. Thus, the comparison of transcriptomic changes in these floral homeotic mutants suggest that OsMADS1 and OsMADS13 may act antagonistically on a common set of genes at early stages of flower development.

Since the "transcription factor activity" ontology term was over-represented in our GO enrichment analysis (**Supplementary Fig. S8A**), putative downstream targets genes encoding for transcriptional regulators were considered for further analyses. To identify likely direct targets, these analyses were limited only to genes with two or more CArG boxes in their putative regulatory regions (3 Kb promoter upstream of Transcription Start Site), untranslated regions (5' and 3' UTRs), gene body (introns and exons). Interestingly, 14% of the DEGs in *osmads13* contain MADS consensus binding

sites which appeared to be bound by OsMADS1 (Khanday et al., 2016; **Dataset III, Supplementary Fig. S8B),** including *APO2*, *OsSPL14* and *bZIP52*.

Zinc-Finger transcription factor mutants to validate dataset

To investigate whether our data could be used to identify genes acting downstream of OsMADS13 and thereby to gain new insights into the regulatory mechanisms underlying gynoecium development in rice, we selected several T-DNA insertion mutants for a preliminary phenotypic analysis. Although the expression profiles of the chosen *OsbHLH* genes suggested a possible role in carpel development, by mutant analysis we could not observe evident phenotypic defects of mutant lines characterised by an insertion in the 5'UTR of *OsbHLH10* (**Supplementary Fig S9A, S9B**), likely due to little effect of T-DNA insertion on gene function. However, a similar T-DNA insertion in the 5'UTR of *OsRAV11* (**Supplementary Fig S9C**) caused gene downregulation and correlated with altered morphology of carpels and seeds in the homozygous mutant (Osnato et al., 2020). Furthermore, insertion mutant lines for two candidate Zinc-Finger transcription factors also showed interesting phenotypes.

The first TF, LOC_Os03g57240 (*ZOS3-19),* is also known as *Drought and Salt Tolerance* (*DST*) and it is closely related to the domestication gene *PROSTRATE GROWTH 1* (*PROG1*, Tan et al., 2008; **Supplementary Fig. S10A**). *DST* encodes a protein belonging to the Cys2/Hys2 (C_2H_2) type Zinc Finger family of TFs constituted by 113 members only in *Oryza sativa subspecies japonica* (ZOS). Despite the high number of related genes in different monocotyledonous plants, this family has undergone significant gene loss events in dicotyledonous plant species. For instance, only the N-terminal region of ZOS3-19/DST exhibits remarkable similarities with few Arabidopsis Zinc-Finger Proteins (AtZFP, **Supplementary Fig. S10B**), such as GIS-like activators of trichome initiation (Gan et al., 2006) and KNUCKLES (KNU, Payne et al., 2004), JAGGED and NUBBIN (JAG and NUB, Dinneny et al., 2006), which are required for reproductive organ development downstream of AG (Gómez-Mena et al., 2005; Sun et al., 2009).

According to the RiceXPro database, *ZOS3-19/DST* is widely expressed throughout plant development, although higher expression levels are observed in leaves and female reproductive tissues (**Supplementary Fig. S10C).** The *ZOS3-19/DST* transcript was strongly up-regulated in the *osmads13* mutant (**Fig. 5A, Supplementary Fig. S10D**), and its cis-regulatory sequences contained several CArG boxes that are bound *in vivo* by OsMADS1 (Khanday et al., 2016). Previous reports indicated that *ZOS3-19/DST* plays several roles in rice development. For example, a mutant

containing an amino acid substitution in the C_2H_2 domain displayed enhanced tolerance to abiotic stresses due to its function controlling stomata functionality during the vegetative phase (Huang et al., 2009). Notably for the same gene, a different point mutation compromising the EAR motif - required for recruitment of co-repressors such as TOPLESS (TPL) and TPL-related proteins - was associated with increased panicle branching and grain number as a consequence of increased cytokinin content in the reproductive meristems (Li et al., 2013). To uncover the effect of *ZOS3-19/DST* loss of function during gynoecium development, we studied a mutant harbouring a T-DNA insertion 109 bp downstream of the ATG, right before the sequence encoding the DNA binding domain (**Fig. 5B; Supplementary Fig. S10E**). Morphological analysis of flowers of the *zos3-19/dst* insertion mutant showed alterations of reproductive organs such as shrunken stamens (normal filament, stunted anthers) and abnormal pistils (**Fig. 5C).** Detailed analyses by Scanning Electron Microscopy (SEM) revealed altered differentiation of basal-apical tissues of the gynoecium, with slender ovaries, reduced style and shortened stigmas (**Fig. 5D**). In addition, histological analysis of mature flowers at anthesis showed that while the wild-type gynoecium developed a bottle-like ovary containing the female gametophyte, this tissue could not be found in the elongated ovary of the mutant gynoecium (**Fig. 5E)**. Consequently, these mutants were completely sterile.

The other locus that we analysed encodes a putative Zinc-Finger Homeo-Domain TF (**Supplementary Fig. S11**), which displays high levels of similarity with Arabidopsis proteins involved in vegetative and reproductive development, including *FLORAL TRANSITION AT THE MERISTEM2* (*FTM2*, Torti et al., 2012). Significant up-regulation of *OsZHD8* was observed in the *osmads13* mutant, especially in the ovule primordia (**Supplementary Fig. S12A-S12C**). To explore its biological role, we studied a mutant characterized by a T-DNA insertion in the 3' UTR of the gene (**Supplementary Fig. S12D-S12F**). Plants carrying this mutation at the homozygous state showed fertility defects which are likely caused by abnormal carpel development, more specifically alterations in the development of the stigma (**Supplementary Fig. S12G**). In addition to a reduced number of seeds, the *oszhd8* mutant also formed smaller panicles with fewer branches as compared to the wild type (**Supplementary Fig. S12H**). These phenotypes are consistent with a possible regulatory role in the control of meristematic activity during reproductive growth and in the correct development of reproductive organs. To conclude, expression analyses and preliminary functional characterisation of insertion mutants allowed us to validate our datasets and the obtained results showed that the data we have generated are a valuable tool to shed new light on the gene regulatory pathways acting downstream of OsMADS13, an important regulator of ovule identity.

Transactivation activity of OsMADS13 tested on candidate downstream genes

The DEGs identified in the *osmads13* mutant could be directly or indirectly controlled by OsMADS13. First, we attempted to generate plants expressing an OsMADS13-GFP fusion protein for ChIP assays. However, the transgenic cassette *ProOsMADS13-OsMADS13(cds)-GFP* (the coding sequence of OsMADS13 under its native promoter) was not able to fully rescue the *osmads13* mutant phenotype, as often a short tracheary element was observed instead of a functional Megaspore Mother Cell (**Supplementary Fig S13A**). We also transformed the mutant with the full *OsMADS13* gene sequence including introns (**Supplementary Fig S13B**) and observed correct localization of the fusion protein (**Supplementary Fig S13C**). However, we were not able to overcome the sterility problems (**Supplemental Fig S13D**). This could be due to the absence of additional regulatory elements in the 3'UTR or distal regions of the promoter, or alternatively to the production of a GFP-tagged version of OsMADS13 which is not fully bioactive.

Therefore, we performed co-transformation assays based on a dual Renilla-Luciferase reporter system to test if OsMADS13 was capable of direct binding to the regulatory regions containing CArG boxes of selected putative downstream genes (*DL, ZOS3-19/DST* and *OsZHD8)*. First, we analysed the genomic sequence of putative targets and identified two regions for each candidate gene, one with and one without the MADS recognition site (schematic representations in **Fig. 6,** details in **Supplementary Fig S14)**. Next, we amplified and cloned the selected fragments upstream of the *LUC* coding sequence to generate the set of reporter vectors to be transiently co-expressed with the effector vector *Pro35S:OsMADS13* in rice protoplasts. Last, we studied the transactivation ability of OsMADS13 on these putative regulatory sequences by measuring the relative expression of *LUC* and *REN* reporter genes in cell lysates. Although we could not find differences in co-transformation assays using sequences related to *OsZHD8* (**Fig. 6A)** and *ZOS3-19* (**Fig. 6B),** we observed a significant decrease in LUC/REN relative transcript levels when OsMADS13 was co-transformed with a reporter vector carrying a fragment of *DL* intron IV containing multiple CArG boxes (**Fig 6C)**, suggesting that *DL*, as carpel specific gene, might be directly targeted for repression by the ovule identity gene OsMADS13.

DISCUSSION

Conservation and diversification of genetic pathways controlling gynoecium development in Arabidopsis and rice

The formation of various floral organs is coordinated by the action and interaction of proteins encoded by members of the *MADS-box* gene family (reviewed by Jack, 2001; Immink et al., 2010; O'Maoileidigh et al., 2014). Interestingly, most of these factors are conserved among flowering plants, although reproductive structures of dicotyledonous and monocotyledonous species display different features.

In the model dicot Arabidopsis, the FM gives rise to four types of floral organs, and the formation of carpel primordia depletes FM activity (Lenhard et al., 2001; Lohmann et al., 2001). Here AG plays a crucial role in repressing stem cell proliferation and promoting the differentiation of reproductive organs (Bowman et al., 1989).

In rice, the C-class factors OsMADS3 and OsMADS58 redundantly control the development of reproductive organs as well as FM determinacy, similarly to Arabidopsis (Dreni et al., 2011). However, the molecular mechanisms leading to the termination of the FM are still poorly understood, partly due to the absence of a functional counterpart of WUS in rice. OsMADS13 is highly similar to the Arabidopsis D-class factor STK, which not only controls ovule identity but also carpel and fruit development (Pinyopich et al., 2003; Mizzotti et al., 2014; Ezquer et al., 2016; Herrera-Ubaldo et al., 2019; Di Marzo et al., 2020). Despite many commonalities, the mechanisms underlying ovule development in these two species are rather different. In Arabidopsis, the FM is completely consumed with the formation of the carpel so that multiple ovule primordia develop from placental tissues derived from the Carpel Margin Meristem (Cucinotta et al., 2014). By way of contrast, in rice a single ovule develops from the placental meristem which derives directly from the inner part of the FM. This means that distinct from Arabidopsis, where STK doesn't necessarily have a meristem determinacy function, in rice OsMADS13 likely contributes to this function as previously shown by the analysis of *osmads13* single mutant and by crossing the *osmads13* mutant with the *osmads3 osmads58* double mutant (Dreni et al., 2007; Dreni et al., 2011).

Similar sets of genes act downstream of AG and OsMADS13

In Arabidopsis, genome-wide approaches revealed that AG directly activates different regulatory factors, including several *MADS-box* genes acting in reproductive growth and three closely related *ARGONAUTE* (*AGO)* genes encoding RNA binding proteins (Ó'Maoiléidigh et al., 2013; Ó'Maoiléidigh

et al., 2018). In addition, AG and SEP proteins converge on the transcriptional regulation of *CRABSCLAW* (*CRC*), a gene encoding a YABBY TF which determines carpel development (Alvarez and Smyth, 1999). Indeed, *CRC* is a direct target of AG (Gómez-Mena et al., 2005), and is ectopically expressed in carpelloid structures of higher order mutants (Brambilla et al., 2007).

In our study, GO enrichment analyses of DEGs unveiled a significant enrichment in transcription regulatory activity in the *osmads13* mutant, in accordance with previous observations for *ag* mutant (Ó'Maoiléidigh et al., 2013). Likewise, similar gene families seem to act downstream of OsMADS13 in rice gynoecium. Indeed, we found up-regulation of the carpel identity genes *OsMADS3, OsMADS58* and *DL*, the rice ortholog of *CRC* (Yamaguchi et al., 2004). Conversely, *OsMEL1,* an *AGO-like* gene essential for germ cell development, is down-regulated in *osmads13*. Nevertheless, the interplay between floral homeotic proteins seems to be more complex in grasses, likely due to the diversification and neo-functionalization of SEP-like and AG-like factors. For example, OsMADS1 mediates the repression of IM identity genes (Khanday et al., 2013) and promotes the early activation of genes involved in floral organ formation (Hu et al., 2015). In addition, OsMADS1 controls FM termination together with OsMADS3 and OsMADS58 but functions on partially independent pathways from *OsMADS13* (Hu et al., 2015). Our comparative transcriptomic analysis suggests that OsMADS1 and OsMADS13 might control the same developmental pathways in an antagonistic manner.

Novel Players may control the balance between meristem maintenance and gynoecium patterning

At the molecular level, the Arabidopsis AG floral homeotic protein controls the termination of FM activity by directly repressing *WUS* (Liu et al., 2011) and activating the transcriptional repressor KNU (Sun et al., 2009; Sun et al., 2014). KNU also regulates the proximo-distal pattern of gynoecium development since ectopic structures resembling stamens and carpels develop from the placenta of *knu* flowers (Payne et al., 2004). Besides *KNU*, other C_2H_2 Zinc Finger TFs are known to act downstream of AG. Specifically, *JAG* and the closely related gene *NUB* redundantly control reproductive growth as their loss of function affects microsporangia development inside the anther and the formation of carpel walls (Dinneny et al., 2006). Strikingly, in *jag nub* mutant ovules are exposed as valve tissues opened in the apical region (Dinneny et al., 2006).

Here we report the preliminary characterization of ZOS3-19/DST, a rice protein which contains a C_2H_2 -type DNA binding domain similar to those of KNU, JAG and NUB. Despite its wide expression pattern throughout plant development, a T-DNA insertion near the ATG causes macroscopic alterations in reproductive organs. In fact, loss of function correlates with wrinkled stamens and

patterning defects of the carpel. Although morphological analysis of the external structure of the latter seems to suggest that the mutant pistil has been correctly differentiated, abnormalities of the internal structure of the gynoecium indicate that the developmental program has stopped before the formation of the female gametophyte. Hence in *zos3-19/dst* mutant flowers, it is plausible that the pool of pluripotent cells of the FM is consumed during carpel development and the differentiation of the pistil along the basal-apical axis does not occur properly, leading to elongated ovary and reduced style-stigmas. Therefore, we propose a function for ZOS3-19/DST controlling the balance between cell proliferation and differentiation. This could be achieved by modifying the hormonal content, in agreement with previous report showing that ZOS3-19/DST regulates the expression of *OsCKX2*, an enzyme responsible for controlling the level of active CKs within developing reproductive tissues (Li et al., 2013). Similarly, defects in gynoecium development and sterility problems were also observed in the *oszhd8* mutant, pointing to a role for this TF at different stages of flower formation. Both mutants showed interesting female reproductive organ phenotypes suggesting that our dataset has utility in identifying new candidate genes downstream of *OsMADS13*.

Testing direct binding of OsMADS13 to putative target genes

Based on expression analyses in reproductive tissues, we propose a role for OsMADS13 as master regulator of key-genes involved in the development of the gynoecium (as depicted in **Fig. 7**). On one hand, "carpel genes" must be switched off in those cells of the FM that would give origin to the OP in the wild type and are de-repressed in the absence of functional OsMADS13. On the other hand, genes involved in gamete development should be activated in the OP during floral organ maturation before meiosis takes place.

Transient transactivation assays in rice protoplasts indicated that OsMADS13 could bind at least the regulatory sequences containing CArG boxes in *DL* intron IV, and to mediate the transcriptional repression of the reporter gene. Despite these promising results, further studies are required to confirm the direct binding of OsMADS13 to other putative targets *in vivo*. Besides, further research using additional mutant alleles for candidate genes, potentially generated by CRISPR-Cas9 technology, will be needed to support these findings.

Author contribution:

M.O. performed most of the experiments, analysed data and prepared graphics; E.L., expression analyses and co-transformation assay; A.G., in situ hybridization and Laser Micro-Dissection; A.P. and L.D., rice transformation and Laser Micro-Dissection; M.C. and D.H., phylogenetic and RNA-sequencing data analyses. M.O. and M.M.K conceived experimental design. M.O., M.M.K. and S.P. wrote the manuscript.

REFERENCE LIST

Agrawal GK, Abe K, Yamazaki M, Miyao A, Hirochika H (2005) Conservation of the E-function for floral organ identity in rice revealed by the analysis of tissue culture-induced loss-of-function mutants of the OsMADS1 gene. Plant Molecular Biology **59**: 125–135

Alvarez J, Smyth DR (1999) CRABS CLAW and SPATULA, two Arabidopsis genes that control carpel development in parallel with AGAMOUS. Development 126: 2377-2386

Balanzà V, Roig-Villanova I, Di Marzo M, Masiero S, Colombo L (2016) Seed abscission and fruit dehiscence required for seed dispersal rely on similar genetic networks. Development 143: 3372-3381; doi: 10.1242/dev.135202

Bowman JL, Smyth DR, Meyerowitz EM (1989) Genes directing flower development in Arabidopsis. The Plant Cell, Vol. 1, 37-52; doi: 10.2307/3869060

Bowman JL, Smyth DR, Meyerowitz EM (2012) The ABC model of flower development: Then and now. Development 139: 4095-4098; doi: 10.1242/dev.083972

Brambilla V, Battaglia R, Colombo M, Masiero S, Bencivenga S, Kater MM, Colombo L (2007) Genetic and molecular interactions between BELL1 and MADS box factors support ovule development in Arabidopsis. The Plant Cell, Vol. 19: 2544–2556. doi: 10.1105/tpc.107.051797

Brand U, Fletcher JC, Hobe M, Meyerowitz EM, Simon R (2000) Dependence of stem cell fate in Arabidopsis on a feedback loop regulated by CLV3 activity. Science. Vol. 289, Issue 5479, pp. 617-619. doi: 10.1126/science.289.5479.617

Causier B, Castillo R, Xue Y, Schwarz-Sommer Z, Davies B (2010) Tracing the evolution of the floral homeotic B-and C-function genes through genome synteny. Molecular Biology and Evolution. doi: 10.1093/molbev/msq156

Cucinotta M, Colombo L, Roig-Villanova I (2014) Ovule development, a new model for lateral organ formation. Frontiers in Plant Science. Volume 5, article 117, pp 1-12. doi: 10.3389/fpls.2014.00117

Cui R, Han J, Zhao S, Su K, Wu F, Du X, Xu Q, Chong K, Theißen G, Meng Z (2010) Functional conservation and diversification of class e floral homeotic genes in rice (Oryza sativa). The Plant Journal 61, 767–781. doi: 10.1111/j.1365-313X.2009.04101.

Di Marzo M, Herrera-Ubaldo H, Caporali E, Novák O, Strnad M, Balanzà V, Ezquer I, Mendes MA, de Folter S, Colombo L (2020) SEEDSTICK Controls Arabidopsis Fruit Size by Regulating Cytokinin Levels and FRUITFULL. Cell Reports. Volume 30, Issue 8, pp 2846-2857.e3. doi: 10.1016/j.celrep.2020.01.101

Dinneny JR, Weigel D, Yanofsky MF (2006) NUBBIN and JAGGED define stamen and carpel shape in Arabidopsis. Development. 133: 1645-1655; doi: 10.1242/dev.02335

Ditta G, Pinyopich A, Robles P, Pelaz S, Yanofsky MF (2004) The SEP4 gene of Arabidopsis thaliana functions in floral organ and meristem identity. Current Biology. 14(21):1935-40. doi: 10.1016/j.cub.2004.10.028

Dreni L, Jacchia S, Fornara F, Fornari M, Ouwerkerk PBF, An G, Colombo L, Kater MM (2007) The D-lineage MADS-box gene OsMADS13 controls ovule identity in rice. The Plant Journal. 52(4):690-9. doi: 10.1111/j.1365-313X.2007.03272.

Dreni L, Pilatone A, Yun D, Erreni S, Pajoro A, Caporali E, Zhang D, Katera MM (2011) Functional analysis of all AGAMOUS subfamily members in rice reveals their roles in reproductive organ identity determination and meristem determinacy. The Plant Cell, Vol. 23: 2850–2863. doi: 10.1105/tpc.111.087007

Egea-Cortines M, Saedler H, Sommer H (1999) Ternary complex formation between the MADS-box proteins SQUAMOSA, DEFICIENS and GLOBOSA is involved in the control of floral architecture in Antirrhinum majus. EMBO Journal 18(19): 5370–5379. doi: 10.1093/emboj/18.19.5370

Ezquer I, Mizzotti C, Nguema-Ona E, Gotté M, Beauzamy L, Viana VE, Dubrulle N, de Oliveira AC, Caporali E, Koroney AS, et al (2016) The developmental regulator SEEDSTICK controls

structural and mechanical properties of the arabidopsis seed coat. The Plant Cell, Vol. 28: 2478–2492. doi: 10.1105/tpc.16.00454

Favaro R, Pinyopich A, Battaglia R, Kooiker M, Borghi L, Ditta G, Yanofsky MF, Kater MM, Colombo L (2003) MADS-Box Protein Complexes Control Carpel and Ovule Development in Arabidopsis. The Plant Cell 15(11): 2603–2611. doi: 10.1105/tpc.015123

Fernández-Calvo P, Chini A, Fernández-Barbero G, Chico JM, Gimenez-Ibanez S, Geerinck J, Eeckhout D, Schweizer F, Godoy M, Franco-Zorrilla JM, et al (2011) The Arabidopsis bHLH transcription factors MYC3 and MYC4 are targets of JAZ repressors and act additively with MYC2 in the activation of jasmonate responses. The Plant Cell, Vol. 23: 701–715. doi: 10.1105/tpc.110.080788

Galbiati F, Sinha Roy D, Simonini S, Cucinotta M, Ceccato L, Cuesta C, Simaskova M, Benkova E, Kamiuchi Y, Aida M, et al (2013) An integrative model of the control of ovule primordia formation. The Plant Journal 76, 446–455. doi: 10.1111/tpj.12309

Gan Y, Kumimoto R, Liu C, Ratcliffe O, Yu H, Broun P (2006) GLABROUS INFLORESCENCE STEMS modulates the regulation by gibberellins of epidermal differentiation and shoot maturation in Arabidopsis. The Plant Cell 18(6): 1383–1395. doi: 10.1105/tpc.106.041533

Gómez-Mena C, de Folter S, Costa MMR, Angenent GC, Sablowski R (2005) Transcriptional program controlled by the floral homeotic gene AGAMOUS during early organogenesis. Development 132(3):429-38. doi: 10.1242/dev.01600

Herrera-Ubaldo H, Lozano-Sotomayor P, Ezquer I, Di Marzo M, Montes RAC, Gomez-Felipe A, Pablo-Villa J, Diaz-Ramirez D, Ballester P, Ferrandiz C, et al (2019) New roles of NO TRANSMITTING TRACT and SEEDSTICK during medial domain development in arabidopsis fruits. Development 146, dev172395, pp 1-14. doi: 10.1242/dev.172395

Honma T, Goto K (2001) Complexes of MADS-box proteins are sufficient to convert leaves into floral organs. Nature 409 (6819):525-9. doi: 10.1038/35054083

Hu Y, Liang W, Yin C, Yang X, Ping B, Li A, Jia R, Chen M, Luo Z, Cai Q, et al (2015) Interactions of OsMADS1 with floral homeotic genes in rice flower development. Molecular Plant Volume 8, Issue 9, pp 1366.1384. doi: 10.1016/j.molp.2015.04.009

Huang XY, Chao DY, Gao JP, Zhu MZ, Shi M, Lin HX (2009) A previously unknown zinc finger protein, DST, regulates drought and salt tolerance in rice via stomatal aperture control. Genes and

Development 23(15):1805-17. doi: 10.1101/gad.1812409

Hugouvieux V, Silva CS, Jourdain A, Stigliani A, Charras Q, Conn V, Conn SJ, Carles CC, Parcy F, Zubieta C (2018) Tetramerization of MADS family transcription factors SEPALLATA3 and AGAMOUS is required for floral meristem determinacy in Arabidopsis. Nucleic Acids Research 46(10):4966-4977. doi: 10.1093/nar/gky205

Ikeda-Kawakatsu K, Maekawa M, Izawa T, Itoh JI, Nagato Y (2012) ABERRANT PANICLE ORGANIZATION 2/RFL, the rice ortholog of Arabidopsis LEAFY, suppresses the transition from inflorescence meristem to floral meristem through interaction with APO1. The Plant Journal 69, 168–180. doi: 10.1111/j.1365-313X.2011.04781.

Immink RGH, Kaufmann K, Angenent GC (2010) The "ABC" of MADS domain protein behaviour and interactions. Seminars in Cell and Developmental Biology Volume 21, Issue 1, Pages 87-93. doi: 10.1016/j.semcdb.2009.10.004

Itoh JI, Nonomura KI, Ikeda K, Yamaki S, Inukai Y, Yamagishi H, Kitano H, Nagato Y (2005) Rice plant development: From zygote to spikelet. Plant and Cell Physiology Volume 46, Issue 1, Pages 23-47**.** doi: 10.1093/pcp/pci501

Jack T (2001) Plant development going MADS. Plant Molecular Biology **46**, pages515–520. doi: 10.1023/A:1010689126632

Jeon JS, Jang S, Lee S, Nam J, Kim C, Lee SH, Chung YY, Kim SR, Lee YH, Cho YG, et al (2000) leafy hull sterile 1 is a homeotic mutation in a rice MADS box gene affecting rice flower development. The Plant Cell 12(6): 871–885. doi: 10.1105/tpc.12.6.871

Jiao Y, Wang Y, Xue D, Wang J, Yan M, Liu G, Dong G, Zeng D, Lu Z, Zhu X, et al (2010) Regulation of OsSPL14 by OsmiR156 defines ideal plant architecture in rice. Nature Genetics **42**, pages 541–544. doi: 10.1038/ng.591

Jung KH, Han MJ, Lee YS, Kim YW, Hwang I, Kim MJ, Kim YK, Nahm BH, An G (2005) Rice Undeveloped Tapetum1 is a major regulator of early tapetum development. The Plant Cell 17(10):2705-22. doi: 10.1105/tpc.105.034090

Kaufmann K, Muiño JM, Jauregui R, Airoldi CA, Smaczniak C, Krajewski P, Angenent GC (2009) Target genes of the MADS transcription factor sepallata3: Integration of developmental and hormonal pathways in the arabidopsis flower. PLoS Biology Volume 7, Issue 4, e1000090, pp 0854-0875. doi: 10.1371/journal.pbio.1000090

Khanday I, Das S, Chongloi GL, Bansal M, Grossniklaus U, Vijayraghavan U (2016) Genome-wide targets regulated by the OsMADS1 transcription factor reveals its DNA recognition properties. Plant Physiology 172(1):372-88. doi: 10.1104/pp.16.00789

Khanday I, Ram Yadav S, Vijayraghavan U (2013) Rice LHS1/UsMADS1 controls floret meristem specification by coordinated regulation of transcription factors and hormone signaling pathways. Plant Physiology 161(4):1970-83. doi: 10.1104/pp.112.212423

Kubo T, Fujita M, Takahashi H, Nakazono M, Tsutsumi N, Kurata N (2013) Transcriptome analysis of developing ovules in rice isolated by laser microdissection. Plant and Cell Physiology Volume 54, Issue 5, Pages 750-765. doi: 10.1093/pcp/pct029

Laux T, Mayer KFX, Berger J, Jürgens G (1996) The WUSCHEL gene is required for shoot and floral meristem integrity in Arabidopsis. Development 122, 87-96.

Lenhard M, Bohnert A, Jürgens G, Laux T (2001) Termination of stem cell maintenance in Arabidopsis floral meristems by interactions between Wuschel and Agamous. Cell Volume 105, Issue 6, Pages 805-814. doi: 10.1016/S0092-8674(01)00390-7

Li H, Liang W, Hu Y, Zhu L, Yin C, Xu J, Dreni L, Kater MM, Zhang D (2011) Rice MADS6 interacts with the floral homeotic genes SUPERWOMAN1, MADS3, MADS58, MADS13, and DROOPING LEAF in specifying floral organ identities and meristem fate. The Plant Cell 23(7):2536-52. doi: 10.1105/tpc.111.087262

Li N, Zhang DS, Liu HS, Yin CS, Li XX, Liang WQ, Yuan Z, Xu B, Chu HW, Wang J, et al (2006) The rice tapetum degeneration retardation gene is required for tapetum degradation and anther development. The Plant Cell Vol. 18, 2999–3014. doi: 10.1105/tpc.106.044107

Li S, Zhao B, Yuan D, Duan M, Qian Q, Tang L, Wang B, Liu X, Zhang J, Wang J, et al (2013) Rice zinc finger protein DST enhances grain production through controlling Gn1a/OsCKX2 expression. Proceedings of the National Academy of Sciences of the United States of America 110 (8) 3167-3172. doi: 10.1073/pnas.1300359110

Liljegren SJ, Ditta GS, Eshed Y, Savidge B, Bowmant JL, Yanofsky MF (2000) SHATTERPROOF MADS-box genes control dispersal in Arabidopsis. Nature 404(6779):766-70. doi: 10.1038/35008089

Liu X, Kim YJ, Müller R, Yumul RE, Liu C, Pan Y, Cao X, Goodrich J, Chen X (2011) AGAMOUS terminates floral stem cell maintenance in arabidopsis by directly repressing WUSCHEL through recruitment of Polycomb Group proteins. The Plant Cell 23(10):3654-70. doi:

10.1105/tpc.111.091538

Lohmann JU, Hong RL, Hobe M, Busch MA, Parcy F, Simon R, Weigel D (2001) A molecular link between stem cell regulation and floral patterning in Arabidopsis. Cell 105(6):793-803. doi: 10.1016/S0092-8674(01)00384-1

Lopez-Dee, M PW, Enrico PË, Rigola D, Buono I Del, Sari M, M GM, Colombo KL (1999) OsMADS13, a novel rice MADS-box gene expressed during ovule development. Developmental Genetics 25(3):237-44. doi: 10.1002/(SICI)1520-6408(1999)25:3<237::AID-DVG6>3.0.CO;2-L.

Malcomber ST, Kellogg EA (2005) SEPALLATA gene diversification: Brave new whorls. Trends in Plant Science 10(9):427-35. doi: 10.1016/j.tplants.2005.07.008

Malcomber ST, Kellogg EA (2004) Heterogenous expression patterns and separate roles of the SEPALLATA gene LEAFY HULL STERILE1 in grasses. The Plant Cell Vol. 16, 1692–1706. doi: 10.1105/tpc.021576

Massari ME, Murre C (2000) Helix-Loop-Helix Proteins: Regulators of Transcription in Eucaryotic Organisms. Molecular and Cellular Biology 20(2): 429–440. doi: 10.1128/mcb.20.2.429-440.2000

Matias-Hernandez L, Battaglia R, Galbiati F, Rubes M, Eichenberger C, Grossniklaus U, Kater MM, Colombo L (2010) VERDANDI is a direct target of the MADS domain ovule identity complex and affects embryo sac differentiation in Arabidopsis. The Plant Cell 22(6):1702-15. doi: 10.1105/tpc.109.068627

Mendes MA, Guerra RF, Berns MC, Manzo C, Masiero S, Finzi L, Kater MM, Colombo L (2013) MADS domain transcription factors mediate short-range DNA looping that is essential for target gene expression in Arabidopsis. The Plant Cell Vol. 25: 2560–2572. doi: 10.1105/tpc.112.108688

Miura K, Ikeda M, Matsubara A, Song XJ, Ito M, Asano K, Matsuoka M, Kitano H, Ashikari M (2010) OsSPL14 promotes panicle branching and higher grain productivity in rice. Nature Genetics **42**, pages545–549. doi: 10.1038/ng.592

Mizzotti C, Ezquer I, Paolo D, Rueda-Romero P, Guerra RF, Battaglia R, Rogachev I, Aharoni A, Kater MM, Caporali E, et al (2014) SEEDSTICK is a Master Regulator of Development and Metabolism in the Arabidopsis Seed Coat. PLoS Genetics Volume 10, Issue 12, e1004856, pp 1-15. doi: 10.1371/journal.pgen.1004856

Moreno-Risueño MA, Van Norman JM, Moreno A, Zhang J, Ahnert SE, Benfey PN (2010) Oscillating gene expression determines competence for periodic Arabidopsis root branching. Science 329(5997):1306-11. doi: 10.1126/science.1191937

Nakata M, Ohme-Takagi M (2013) Two bHLH-type transcription factors, JA-ASSOCIATED MYC2-LIKE2 and JAM3, are transcriptional repressors and affect male fertility. Plant Signalling & Behaviour 8(12): e26473-1 to e26473-4. doi: 10.4161/psb.26473

Nonomura KI, Morohoshi A, Nakano M, Eiguchi M, Miyao A, Hirochika H, Kurataa N (2007) A germ cell-specific gene of the ARGONAUTE family is essential for the progression of premeiotic mitosis and meiosis during sporogenesis in rice. The Plant Cell Vol. 19: 2583–2594. doi: 10.1105/tpc.107.053199

Ó'Maoiléidigh DS, Stewart D, Zheng B, Coupland G, Wellmer F (2018) Floral homeotic proteins modulate the genetic program for leaf development to suppress trichome formation in flowers. Development 145, dev157784, pages 1-12. doi: 10.1242/dev.157784

O'Maoileidigh DS, Graciet E, Wellmer F (2014) Genetic Control of Arabidopsis Flower Development. Advances in Botanical Research Volume 72, Pages 159-190. doi: 10.1016/B978-0-12-417162-6.00006-7

Ó'Maoiléidigh DS, Wuest SE, Rae L, Raganelli A, Ryan PT, Kwaśniewska K, Das P, Lohan AJ, Loftus B, Graciet E, et al (2013) Control of reproductive floral organ identity specification in arabidopsis by the C function regulator AGAMOUS. The Plant Cell 25(7):2482-503. doi: 10.1105/tpc.113.113209

Osnato M, Matias-Hernandez L, Aguilar-Jaramillo AE, Kater MM and Pelaz S. (2020). Genes of the RAV Family Control Heading Date and Carpel Development in Rice. Plant Physiology Vol. 183, pp. 1663–1680. doi: 10.1104/pp.20.00562

Payne T, Johnson SD, Koltunow AM (2004) KNUCKLES (KNU) encodes a C2H2 zinc-finger protein that regulates development of basal pattern elements of the Arabidopsis gynoecium. Development 131: 3737-3749. doi: 10.1242/dev.01216

Pelaz S, Ditta GS, Baumann E, Wisman E, Yanofsky MF (2000) B and C floral organ identity functions require SEPALLATTA MADS-box genes. Nature 405(6783):200-3. doi: 10.1038/35012103

Pinyopich A, Ditta GS, Savidge B, Liljegren SJ, Baumann E, Wisman E, Yanofsky MF (2003) Assessing the redundancy of MADS-box genes during carpel and ovule development. Nature **424**, pages

85–88. doi: 10.1038/nature01741

Prasad K, Parameswaran S, Vijayraghavan U (2005) OsMADS1, a rice MADS-box factor, controls differentiation of specific cell types in the lemma and palea and is an early-acting regulator of inner floral organs. The Plant Journal 43(6):915-28. doi: 10.1111/j.1365-313X.2005.02504.

Prasad K, Sriram P, Santhosh Kumar C, Kushalappa K, Vijayraghavan U (2001) Ectopic expression of rice OsMADS1 reveals a role in specifying the lemma and palea, grass floral organs analogous to sepals. Development Genes and Evolution 211(6):281-90. doi: 10.1007/s004270100153

Sasaki-Sekimoto Y, Jikumaru Y, Obayashi T, Saito H, Masuda S, Kamiya Y, Ohta H, Shirasu K (2013) Basic helix-loop-helix transcription factors JASMONATE-ASSOCIATED MYC2-LIKE1 (JAM1), JAM2, and JAM3 are negative regulators of jasmonate responses in Arabidopsis. Plant Physiology 163(1):291-304. doi: 10.1104/pp.113.220129

Schoof H, Lenhard M, Haecker A, Mayer KFX, Jürgens G, Laux T (2000) The stem cell population of Arabidopsis shoot meristems is maintained by a regulatory loop between the CLAVATA and WUSCHEL genes. Cell Volume 100, Issue 6, Pages 635-644. doi: 10.1016/S0092-8674(00)80700-X

Sun B, Looi LS, Guo S, He Z, Gan ES, Huang J, Xu Y, Wee WY, Ito T (2014) Timing mechanism dependent on cell division is invoked by Polycomb eviction in plant stem cells. Science Vol. 343, Issue 6170, 1248559. doi: 10.1126/science.1248559

Sun B, Xu Y, Ng KH, Ito T (2009) A timing mechanism for stem cell maintenance and differentiation in the Arabidopsis floral meristem. Genes and Development 23(15):1791-804. doi: 10.1101/gad.1800409

Tan L, Li X, Liu F, Sun X, Li C, Zhu Z, Fu Y, Cai H, Wang X, Xie D, et al (2008) Control of a key transition from prostrate to erect growth in rice domestication. Nature Genetics 40(11):1360-4. doi: 10.1038/ng.197

Tang X, Zhang ZY, Zhang WJ, Zhao XM, Li X, Zhang D, Liu QQ, Tang WH (2010) Global gene profiling of laser-captured pollen mother cells indicates molecular pathways and gene subfamilies involved in rice meiosis. Plant Physiology 154(4):1855-70. doi: 10.1104/pp.110.161661

Taoka KI, Ohki I, Tsuji H, Furuita K, Hayashi K, Yanase T, Yamaguchi M, Nakashima C, Purwestri YA, Tamaki S, et al (2011) 14-3-3 proteins act as intracellular receptors for rice Hd3a florigen. Nature **476**, pages 332–335. doi: 10.1038/nature10272

Theissen G, Melzer R (2007) Molecular mechanisms underlying origin and diversification of the angiosperm flower. Annals of Botany 100(3): 603–619. doi: 10.1093/aob/mcm143

Theißen G, Saedler H (2001) Floral quartets. Nature. **409**, pages 469–471 doi: 10.1038/35054172

Torti S, Fornara F, Vincent C, Andres F, Nordstrom K, Gobel U, Knoll D, Schoof H, Coupland G (2012) Analysis of the Arabidopsis Shoot Meristem Transcriptome during Floral Transition Identifies Distinct Regulatory Patterns and a Leucine-Rich Repeat Protein That Promotes Flowering. The Plant Cell **24**: 444–462. doi/10.1105/tpc.111.092791

Yamaguchi N, Huang J, Xu Y, Tanoi K, Ito T (2017) Fine-tuning of auxin homeostasis governs the transition from floral stem cell maintenance to gynoecium formation. Nature Communications **8**, Article number 1125, pp 1-15. doi: 10.1038/s41467-017-01252-6

Yamaguchi T, Lee DY, Miyao A, Hirochika H, An G, Hirano HY (2006) Functional diversification of the two C-class MADS box genes OSMADS3 and OSMADS58 in Oryza sativa. The Plant Cell Vol. 18, 15–28. doi: 10.1105/tpc.105.037200

Yamaguchi T, Nagasawa N, Kawasaki S, Matsuoka M, Nagato Y, Hirano HY (2004) The Yabby Gene Drooping Leaf Regulates Carpel Specification and Midrib Development in Oryza sativa. The Plant Cell 16(2): 500–509. doi: 10.1105/tpc.018044

Figure Legends

Figure 1. GO annotation and Classification of Differentially Expressed Genes in *osmads13*. (A) 10X10 dot plot representing the classification of DEGs in *osmads13* in sequences related to transposons and retrotransposons (black), expressed genes encoding proteins with unknown function (light grey), genes encoding proteins with annotated function (dark grey). (B) 10X10 dot plot representing the annotation of DEGs in functional categories with percentage as follows: components of metabolic pathways (green); proteins able to bind DNA, RNA and chromatin (red); factors (chaperons, protein modifiers and regulatory enzymes) able to bind proteins (orange); structural components (cell wall and membrane, cytoskeleton) and proteins involved in cell cycle (yellow); factors involved in the response to endogenous and exogenous stimuli (white). (C) GO analysis for molecular function of DEGs in *osmads13* showing over-representation of the categories *binding* and *transcription regulator activity,* and under-representation of the category *catalytic activity*. In white, Data Set I; in green, reference transcriptome (Rice MSU7.0 nonTE transcript ID). (D) Chart showing the percentage of genes encoding single families of TFs in Data Set I (81/464, in white) and in the rice genome (2384[a]/39045[b], in green). APETALA2 (AP2/ERF), Zinc-Finger (ZF), MYB, Homeo-Domain (HD), basic Helix-Loop-Helix (bHLH), basic leucine Zipper (bZIP), No Apical Meristem (NAM) and Heat Shock Transcription Factors (HSF). The remaining 14% are single members of other families. The information was retrieved from the Database of Rice Transcription Factors (a) and Rice Genome Annotation Project (b).

Figure 2. Expression analysis of known regulators of gynoecium development. (A) and (B) Relative expression levels of the ovule identity gene *OsMADS13* and the carpel marker gene *DL* in FM and OP of wild-type (white) and *osmads13* mutant (green). (C) and (D) Up-regulation of *OsMADS3* and *OsMADS8* in FM and OP of *osmads13* mutant. (E) Down-regulation of *APO2* and *OsMEL1* in OP of *osmads13* mutant. Expression data are represented as the mean values of three biological replicates ±SD. Differences were analyzed using Student's t-test and asterisks indicate statistical significance (*P <0.033; **P <0.002; ***P <0.001). *Rice Elongation Factor 1* (*OsEF1*) was used for normalization.

Figure 3. Validation of RNA-seq in developing inflorescences and ovule primordia. Relative expression levels *OsbZIP52*, *HSF* and *HSP* genes in inflorescence (A) and OP (B) of wild type (white) and *osmads13* mutant (green). (C) Schematic representation of alternative transcripts of *OsbHLH6* and specific primers used to amplify the common 3'end (black arrowheads, left) or the shorter transcript (white arrowheads, right). (D) and (E) Differential expression of transcripts variants of *OsbHLH6* in inflorescence and OP. (F) and (G) Relative expression levels of *OsbHLH10* and *OsbHLH39* in inflorescences and OP. Expression data are presented as mean values of three biological replicates

±SD. Differences were analyzed using Student's t-test and asterisks indicate statistical significance (*P < 0.033; **P < 0.002; ***P < 0.001). *OsEF1* and *OsUBQ* were used for normalization.

Figure 4. Comparison of the transcriptome changes of *osmads13* and *OsMADS1 l*oss of function mutant inflorescences. (A) and (B) Modified Venn diagrams showing common and specific differentially expressed genes in *osmads13* (5-8 mm inflorescences, green), *OsMADS1-RNAi* (4- 50 mm inflorescences, red) and *osmads1-z* (5-7 mm inflorescences, yellow). (C) Over-representation of the categories *response to endogenous stimulus* and *signal transduction* in group I (genes upregulated in *osmads13* and downregulated in *osmads1)*. (D) Over-representation of the categories *photosynthesis* and *generation of precursor metabolites and energy* in group II (genes downregulated in *osmads13* and upregulated in *osmads1*). Singular Enrichment Analysis (SEA) for molecular function was carried out using Rice (*Oryza sativa Japonica)* MSU7.0 nonTE transcript ID as Reference in AgriGO.

Figure 5. Molecular and phenotypic analysis of *ZOS3-19/DST*. (A) Upregulation of *ZOS3-19/DST* in immature inflorescences, FM and OP of *osmads13* (green) compared to wild-type (white). Expression data are presented as the mean values of three biological replicates ±SD. Differences were analyzed using Student's t-test and asterisks indicate statistical significance (*P < 0.033; ***P < 0.001). (B) Schematic representation of *ZOS3-19* gene, with T-DNA insertion (yellow triangle) 109 bp down-stream of the ATG, just before the sequence encoding the Zinc Finger domain (from nt 149 to nt 228 bp, corresponding to aa 49 to aa 76). In black, 906 bp coding sequence; in white, 3' UTR; in grey, promoter; in pink, CArG boxes; bar,1 Kb. (C) Morphological analysis by optical microscopy of floral organs (top) and carpels (bottom) of wild type and *zos3-19/dst* mutant. Bar, 1 mm. (D) and (E) Morphological analysis by Scanning Electron Microscopy and histological analysis by longitudinal thin sections (false-colored in grey) showing wild type and *zos3-19/ dst* gynoecia dissected from mature flowers at anthesis. Bar, 0.5 mm.

Figure 6. Interaction between OsMADS13 and putative targets. (A) to (C) Transactivation activity of OsMADS13 in transiently transformed protoplasts, reported as ratio of transcript levels of *LUC* and *REN* reporter genes, relative to *UBQ*. The expression of *LUC* is driven by putative regulatory sequences or coding sequences of *OsZHD8* (A), *DST/ZOS3-19* (B) and *DL* (C). Arrows represent primers used to amplify different fragments of putative downstream genes, with (in orange) or without (in grey) MADS binding sites. In black, coding sequence; in white, UTR; in grey, promoter; orange boxes, CArG sequences.

Figure 7. Molecular mechanisms controlled by AG in Arabidopsis and OsMADS13 in rice. In Arabidopsis, AG controls the termination of FM by directly and indirectly repressing WUS, and activates genes involved in carpel development (top). In wild type flowers, two fused carpels (in violet) containing ovule primordia (in pink) develop in the innermost whorl (bottom). Stamens (yellow), petals (grey) and sepals (green) develop in outer whorls. In rice, OsMADS13 might control the termination of FM indirectly by modulating hormone content and prevents the expression of genes involved in carpel formation in developing ovules (top). In wild type flowers, the pistil (in violet) containing a single ovule primordium (in pink) develops in the innermost whorl (bottom). Stamens (yellow), lodicules (grey) and glumes (green) develop in outer whorls.

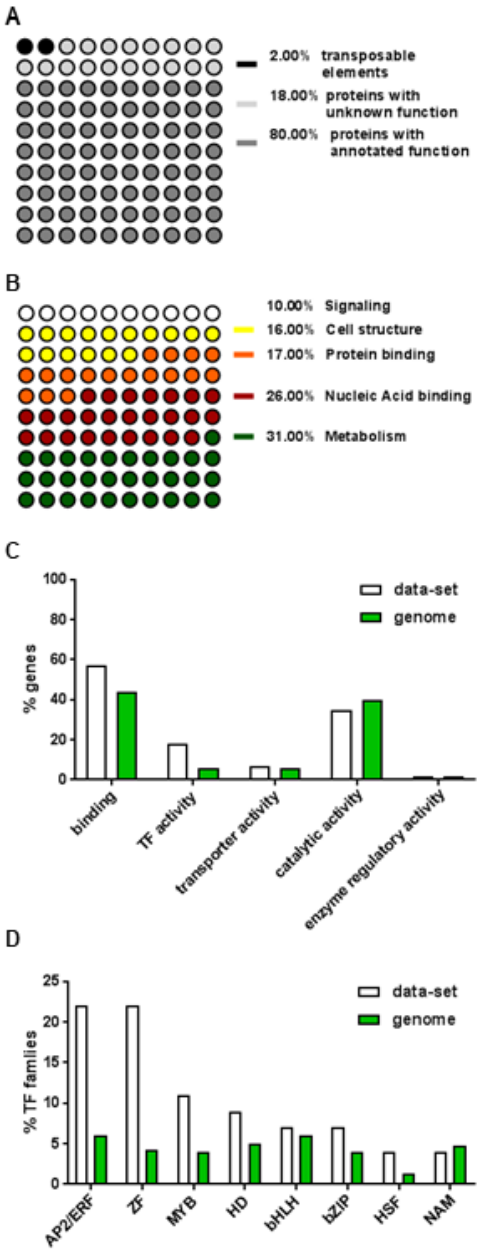

Figure 1. GO annotation and Classification of Differentially Expressed Genes in *osmads13*. (A) 10X10 dot plot representing the classification of DEGs in *osmads13* in sequences related to transposons and retrotransposons (black), expressed genes encoding proteins with unknown function (light grey), genes encoding proteins with annotated function (dark grey). (B) 10X10 dot plot representing the annotation of DEGs in functional categories with percentage as follows: components of metabolic pathways (green); proteins able to bind DNA, RNA and chromatin (red); factors (chaperons, protein modifiers and regulatory enzymes) able to bind proteins (orange); structural components (cell wall and membrane, cytoskeleton) and proteins involved in cell cycle (yellow); factors involved in the response to endogenous and exogenous stimuli (white). (C) GO analysis for molecular function of DEGs in *osmads13* showing over-representation of the categories *binding* and *transcription regulator activity,* and under-representation of the category *catalytic activity*. In white, Data Set I; in green, reference transcriptome (Rice MSU7.0 nonTE transcript ID). (D) Chart showing the percentage of genes encoding single families of TFs in Data Set I (81/464, in white) and in the rice genome (2384[a]/39045[b], in green). APETALA2 (AP2/ERF), Zinc-Finger (ZF), MYB, Homeo-Domain (HD), basic Helix-Loop-Helix (bHLH), basic leucine Zipper (bZIP), No Apical Meristem (NAM) and Heat Shock Transcription Factors (HSF). The remaining 14% are single members of other families. The information was retrieved from the Database of Rice Transcription Factors (a) and Rice Genome Annotation Project (b).

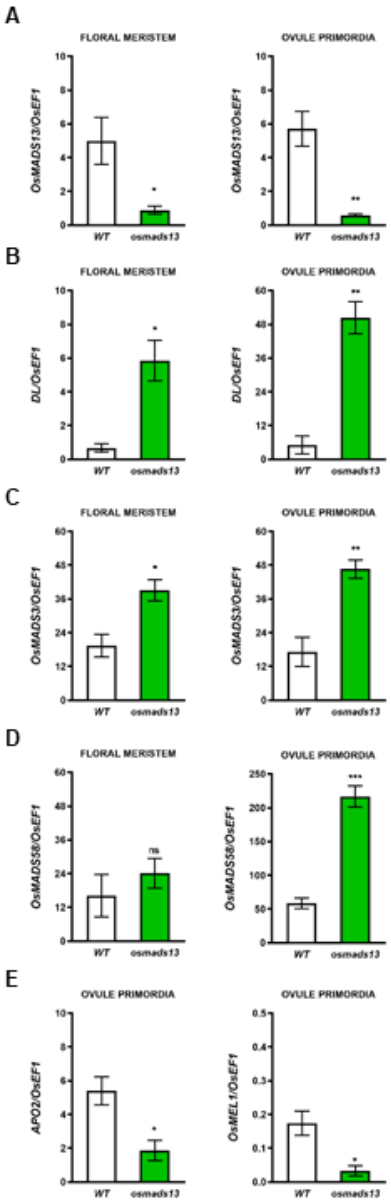

Figure 2. Expression analysis of known regulators of gynoecium development. (A) and (B) Relative expression levels of the ovule identity gene *OsMADS13* and the carpel marker gene *DL* in FM and OP of wild-type (white) and *osmads13* mutant (green). (C) and (D) Up-regulation of *OsMADS3* and *OsMADS8* in FM and OP of *osmads13* mutant. (E) Down-regulation of *APO2* and *OsMEL1* in OP of *osmads13* mutant. Expression data are represented as the mean values of three biological replicates ±SD. Differences were analyzed using Student's t-test and asterisks indicate statistical significance (*P <0.033; **P <0.002; ***P <0.001). *Rice Elongation Factor 1* (*OsEF1*) was used for normalization.

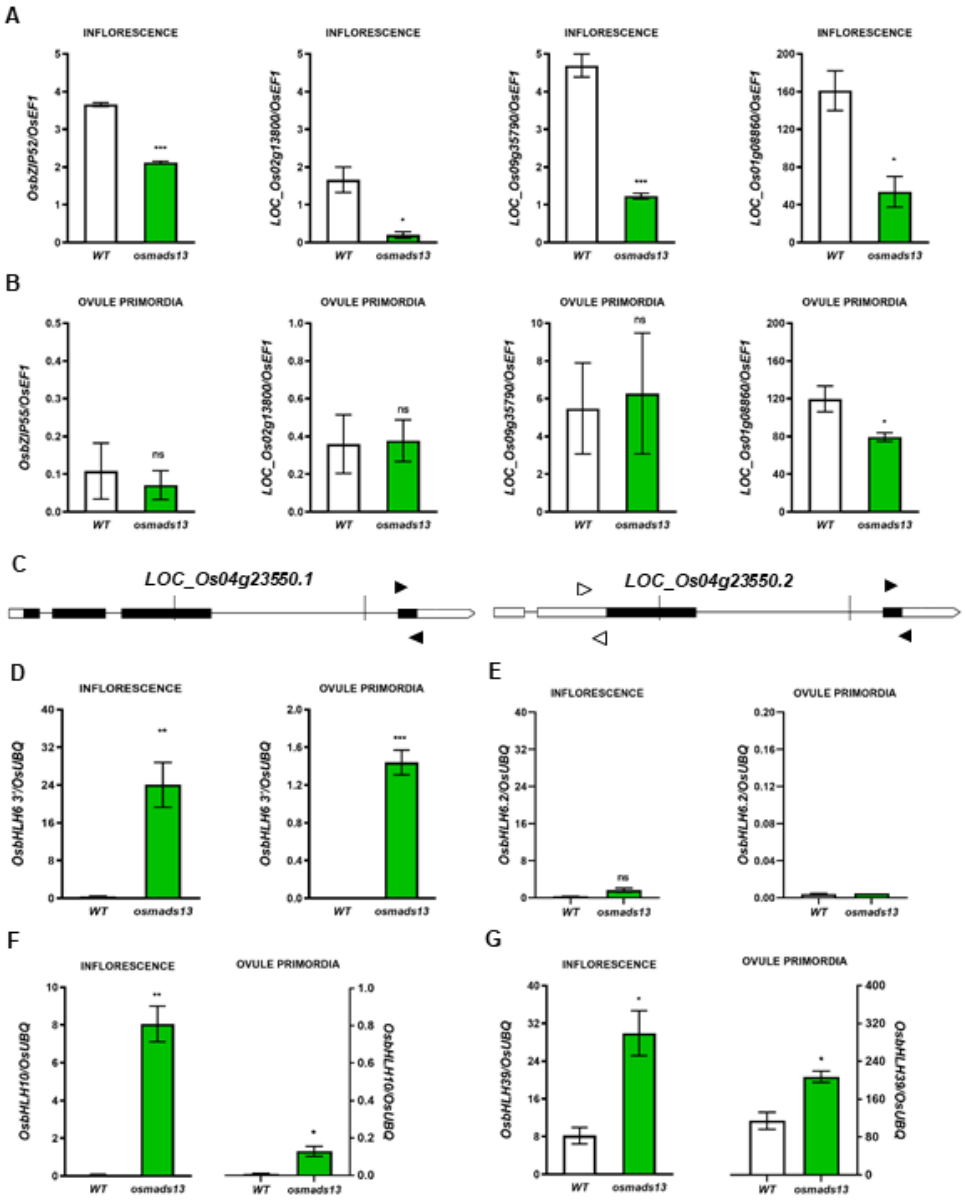

Figure 3. Validation of RNA-seq in developing inflorescences and ovule primordia. Relative expression levels *OsbZIP52*, *HSF* and *HSP* genes in inflorescence (A) and OP (B) of wild type (white) and *osmads13* mutant (green). (C) Schematic representation of alternative transcripts of *OsbHLH6* and specific primers used to amplify the common 3'end (black arrowheads, left) or the shorter transcript (white arrowheads, right). (D) and (E) differential expression of transcripts variants of *OsbHLH6* in inflorescence and OP. (F) and (G) Relative expression levels of *OsbHLH10* and *OsbHLH39* in inflorescences and OP. Expression data are presented as mean values of three biological replicates ±SD. Differences were analyzed using Student's t-test and asterisks indicate statistical significance (*P < 0.033; **P < 0.002; ***P < 0.001). *OsEF1* and *OsUBQ* were used for normalization.

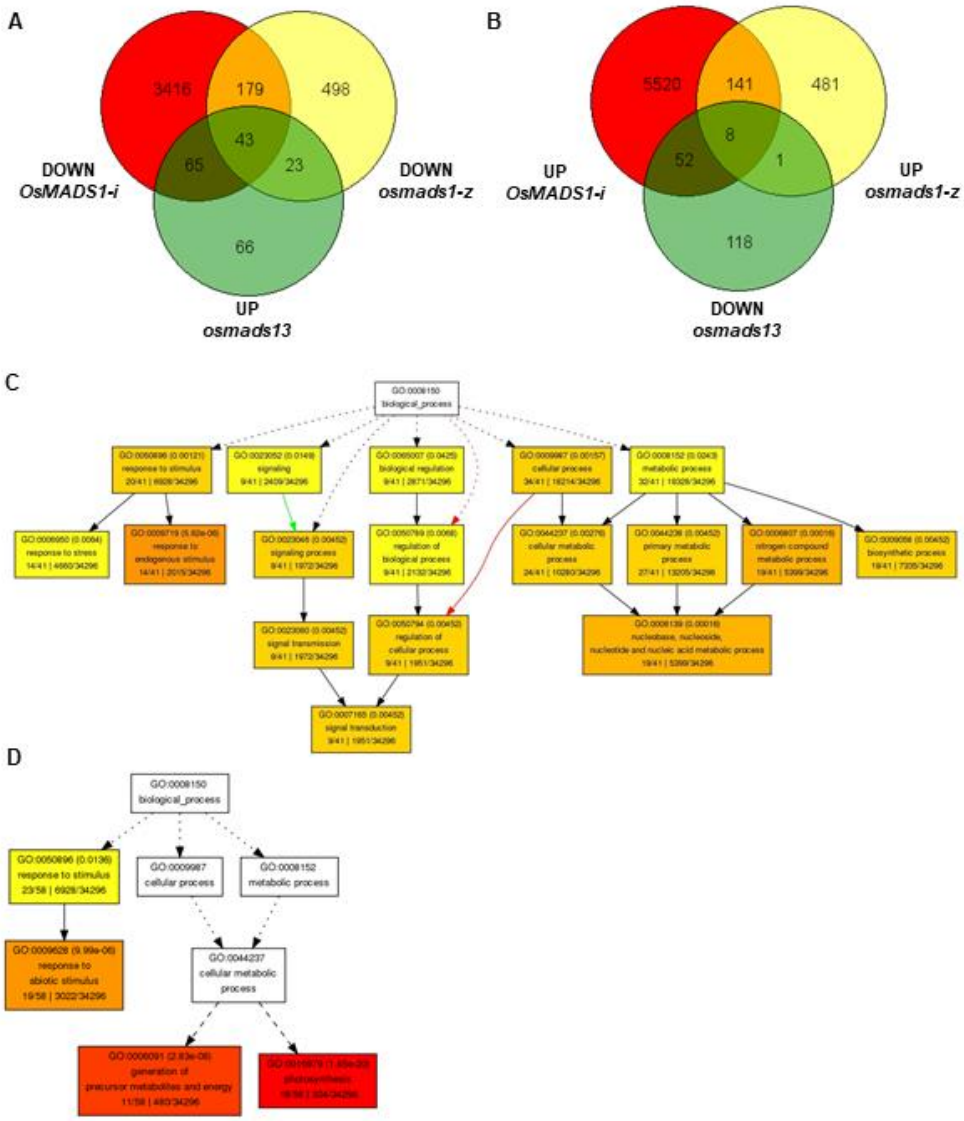

Figure 4. Comparison of the transcriptome changes of *osmads13* and *OsMADS1 l*oss of function mutant inflorescences. (A) and (B) Modified Venn diagrams showing common and specific differentially expressed genes in *osmads13* (5-8 mm inflorescences, green), *OsMADS1-RNAi* (4-50 mm inflorescences, red) and *osmads1-z* (5-7 mm inflorescences, yellow). (C) Over-representation of the categories *response to endogenous stimulus* and *signal transduction* in group I (genes upregulated in *osmads13* and downregulated in *osmads1).* (D) Over-representation of the categories *photosynthesis* and *generation of precursor metabolites and energy* in group II (genes downregulated in *osmads13* and upregulated in *osmads1*). Singular Enrichment Analysis (SEA) for molecular function was carried out using Rice (*Oryza sativa Japonica)* MSU7.0 nonTE transcript ID as Reference in AgriGO.

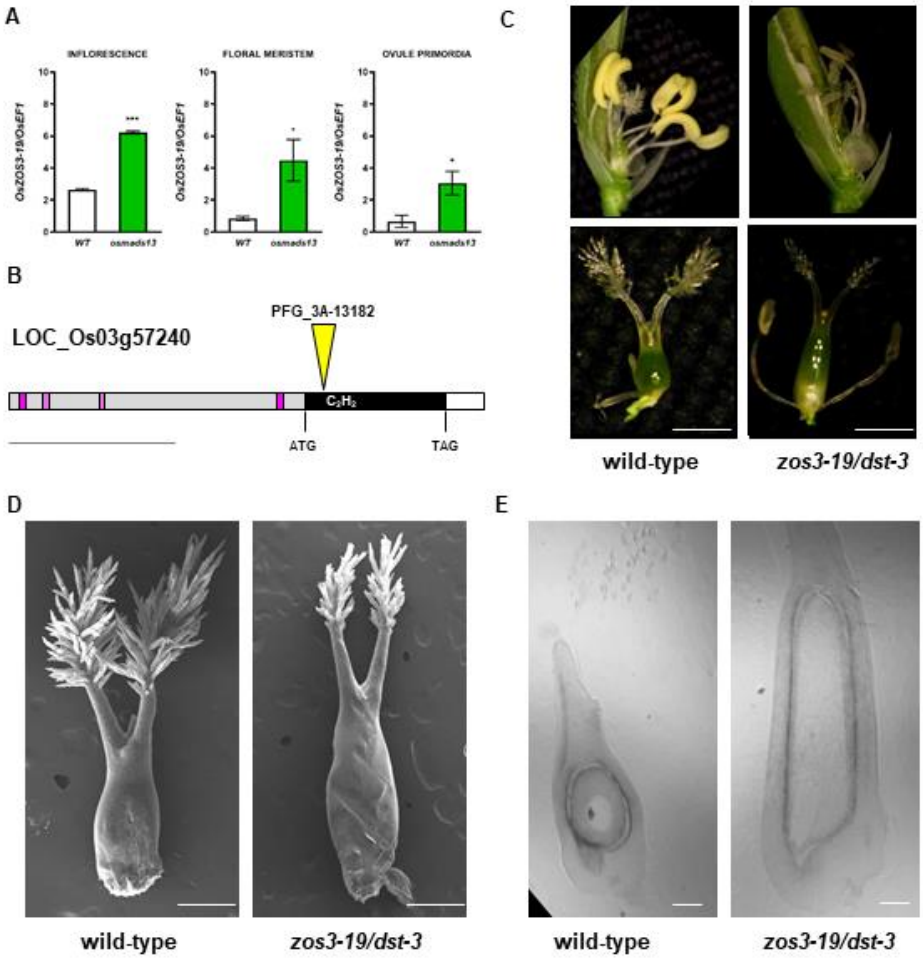

Figure 5. Molecular and phenotypic analysis of *ZOS3-19/DST*. (A) Upregulation of *ZOS3-19/DST* in immature inflorescences, FM and OP of *osmads13* (green) compared to wild-type (white). Expression data are presented as the mean values of three biological replicates ±SD. Differences were analyzed using Student's t-test and asterisks indicate statistical significance (*P < 0.033; ***P < 0.001). (B) Schematic representation of *ZOS3-19* gene, with T-DNA insertion (yellow triangle) 109 bp down-stream of the ATG, just before the sequence encoding the Zinc Finger domain (from nt 149 to nt 228 bp, corresponding to aa 49 to aa 76). In black, 906 bp coding sequence; in white, 3' UTR; in grey, promoter; in pink, CArG boxes; bar,1 Kb. (C) Morphological analysis by optical microscopy of floral organs (top) and carpels (bottom) of wild type and *zos3-19/dst* mutant. Bar, 1 mm. (D) and (E) Morphological analysis by Scanning Electron Microscopy and histological analysis by longitudinal thin sections (false-colored in grey) showing wild type and *zos3-19/ dst* gynoecia dissected from mature flowers at anthesis. Bar, 0.5 mm.

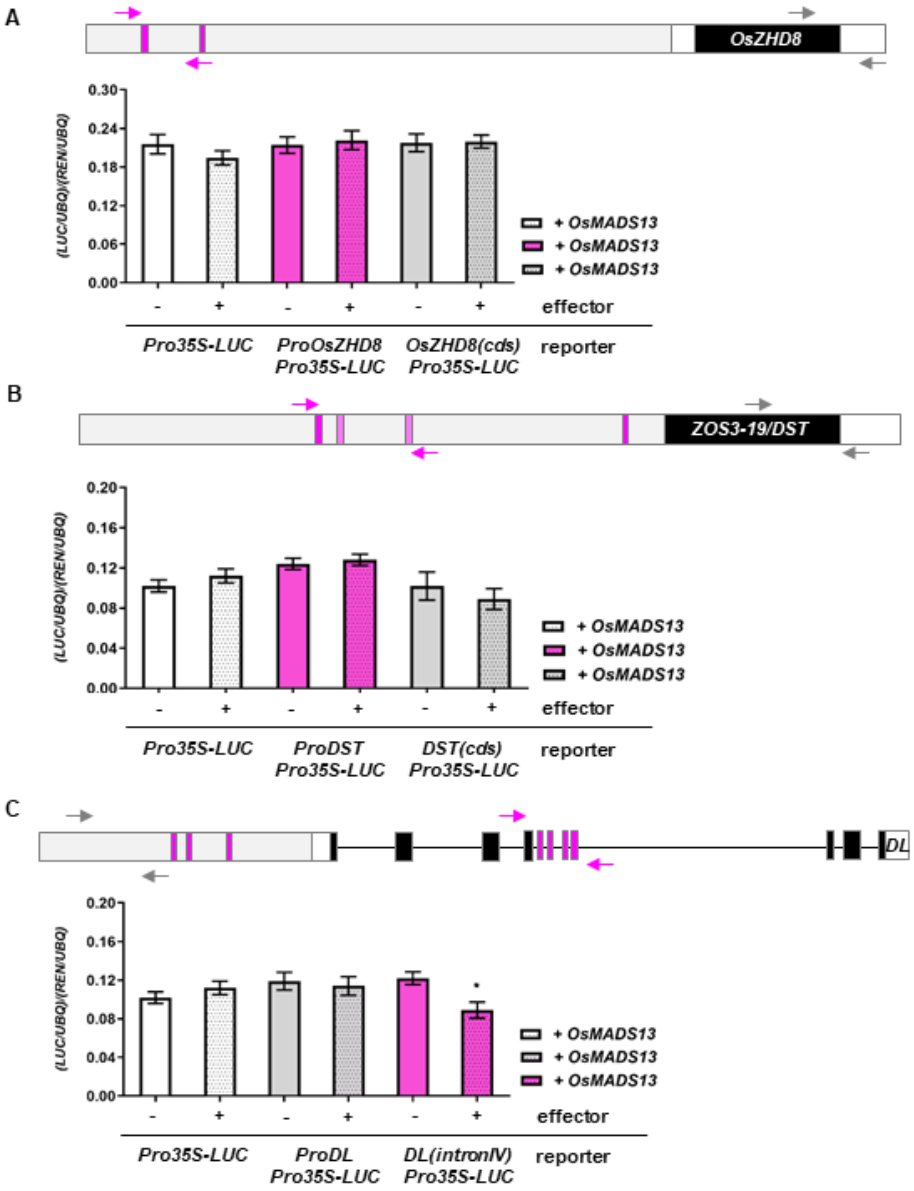

Figure 6. Interaction between OsMADS13 and putative targets. (A) to (C) Transactivation activity of OsMADS13 in transiently transformed protoplasts, reported as ratio of transcript levels of *LUC* and *REN* reporter genes, relative to *UBQ*. The expression of *LUC* is driven by putative regulatory sequences or coding sequences of *OsZHD8* (A), *DST/ZOS3-19* (B) and *DL* (C). Arrows represent primers used to amplify different fragments of putative downstream genes, with (in orange) or without (in grey) MADS binding sites. In black, coding sequence; in white, UTR; in grey, promoter; orange boxes, CArG sequences.

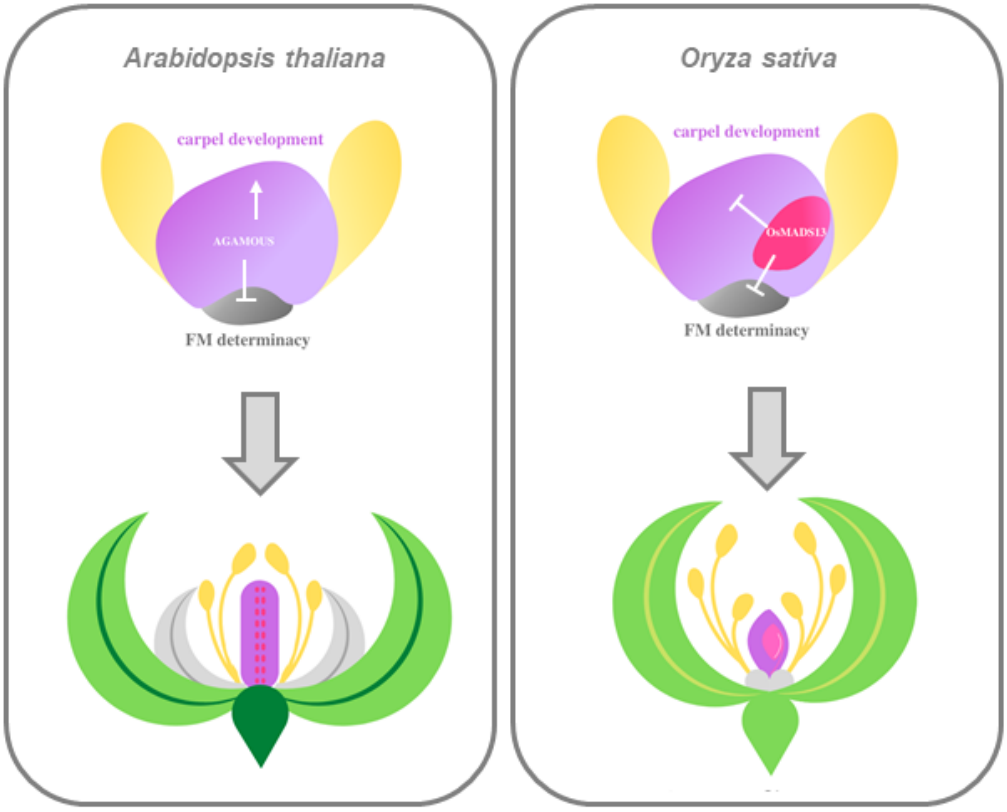

Figure 7. Molecular mechanisms controlled by AG in Arabidopsis and OsMADS13 in rice. In Arabidopsis, AG controls the termination of FM by directly and indirectly repressing WUS, and activates genes involved in carpel development (top). In wild type flowers, two fused carpels (in violet) containing ovule primordia (in pink) develop in the innermost whorl (bottom). Stamens (yellow), petals (grey) and sepals (green) develop in outer whorls. In rice, OsMADS13 might control the termination of FM indirectly by modulating hormone content and prevents the expression of genes involved in carpel formation in developing ovules (top). In wild type flowers, the pistil (in violet) containing a single ovule primordium (in pink) develops in the innermost whorl (bottom). Stamens (yellow), lodicules (grey) and glumes (green) develop in outer whorls.